Materials Research Proceedings 30 (2023) 91-99 https://doi.org/10.21741/9781644902578-13

Canine hindlimb prosthetic research and its manufacturing with the help of additive technology

Michał Kowalik[1,a*], Malwina Ewa Kołodziejczak[2,b], Michał Staniszewski[1], Mateusz Papis[1,c] and Witold Rządkowski[1,d]

[1]Institute of Aeronautics and Applied Mechanics, Faculty of Power and Aeronautical Engineering, Warsaw University of Technology, Nowowiejska 24, Warsaw, Poland

[2]Faculty of National Security, War Studies University, av. Antoniego Chruściela 103, Warsaw, Poland

[a]Michal.Kowalik@pw.edu.pl, [b]m.kolodziejczak@akademia.mil.pl, [c]Mateusz.Papis@pw.edu.pl, [d]Witold.Rzadkowski@pw.edu.pl

Keywords: Endoprosthesis, FEM Analysis, 3D Printing, Safety

Abstract. The purpose of this article is to develop a model and study an English bulldog endoprosthesis made with the help of additive techniques. An analysis of the literature shows the lack of such studies, including both additive techniques and topological optimization of prostheses. Before starting the actual study, general objectives were developed, which took into account the following: prosthesis assembly, fabrication technologies, fabrication conditions, shape, and range of work of the prosthesis. The dimensions of the prosthesis were identified based on the characteristics of the breed - the English bulldog. In the next step, the technology and construction materials were selected. The modeling of the prosthesis was based on the parameterization of dimensions. The parameters were linked by a skeletal model. Also, the objectives necessary to determine the factor of safety were defined. Boundary conditions were determined for the purpose of numerical calculations. The results in the form of reduced stresses and displacement distributions were presented on the maps. In the next part, topological optimization was performed, assuming the high stiffness of the system. Reduced stress maps and displacement distributions were generated for these results with the help of the FEM method. Validation of numerical calculations with real ones was performed.

Introduction

The Animal Protection Bill [1] as well as the EU directives point out that an animal is a living being capable of feeling pain and suffering. Man owes it respect, protection, and care. The animal should be treated humanely, that is, in such a way that ensures that its existential needs are met. In special cases, it is possible to kill the animal immediately. This possibility applies when an animal endures suffering and pain. Man must reduce the suffering of the animals and ensure their normal functioning [2]. One of the ways, in the case of dysfunctions connected with mobility, is the prosthetics. By applying modern manufacturing technologies [3], such as additive technology, it is possible to quickly and cheaply make individual prosthetics designed for a certain breed and even an individual animal [4]. It has also been found that when used for dogs, the endoprosthesis can prolong their lifespan [5].

The literature on the subject presents research on endoprostheses for dogs, made of various construction materials. One of the first endoprostheses design solutions was made of metal - a titanium-nickel prosthesis [6]. The simplest solutions present endoprosthesis as a metal monolith [7]. Other solutions include titanium endoprosthesis, made with a laser powder bed synthesis system, whereas, the cutting guides are made of ABS in a fusion deposition modeling system [8]. Not long ago, additive technologies started to be used to print this type of element (additive

manufacturing) – 3D print [9], [10]. The literature fails to provide an additive manufacturing approach to animal prostheses that would apply topological optimization and their comparative studies. This paper presents it as a scientific innovation.

The purpose of this article is to develop a model and study an English bulldog endoprosthesis made with the help of additive techniques.

General objectives applicable to the conducted research

The model of the prosthesis will be limited by the research objectives. It was assumed that:

- the prosthesis is assembled to an endoprosthesis with a protruding stem ending in a thread or quick-connect;
- the prosthesis is made of plastic and printed by a 3D printer;
- the prosthesis is made in non-laboratory or industrial conditions;
- the material behaves isotropically;
- it should be easy to disassemble the limb replacement for maintenance purposes (e.g. cleaning);
- the shape of the limb is parameterized, that is, the shape is adaptable to the set overall dimensions of the bone (length of the femur, tibia, and metatarsus);
- the limb works on a single plane;
- the prosthesis is printed by a printer with a working scope of 220x220x230 mm;
- the prosthesis is waterproof;
- easily fixed;
- easily cleaned.

Due to the large breed diversity and the associated variation in the skeletal system of dogs, it is not possible to design a single prosthesis for all species [11], [12]. Therefore, for the purpose of this study, it was assumed that the prosthesis will be designed for the English bulldog. This dog breed is particularly prone to hip dysplasia, which requires endoprosthesis [13], [14]. The following dog characteristic was applied: weight 23-25 kg, height ca. 40 cm. As regards the shape of the hindlimbs, they are very muscular along their entire length, slightly shorter than the forelimbs. Knees are pointing slightly outward, ankle joints are small with a small angular range, and the paws are round and compact. Gait characteristics are as follows: short, quick steps, hind paws are not lifted high, on the contrary, they are low-lifted, almost gliding on the ground.

Prosthesis manufacturing technology and selected materials

The choice of prosthesis manufacturing technology depends on surface quality, mechanical strength, and material used. Because of the printed material, LOM (Laminated Object Manufacturing) technology has been ruled out [15], as the prosthesis cannot be made of paper, due to its poor strength properties as well as no water resistance, which then leads to a lack of durability. Among the technologies discussed, those that use other materials for printing purposes include SLS, FDM, and SLA. Analyzing the advantages and disadvantages of the aforementioned technologies, FDM technology was selected as preferable in this project because it is popular and available on the market, hence the lower costs in the case of mass production. The second argument behind choosing this method is the possibility to print large sizes, and thus produce monoliths.

Due to the high mechanical strength and increased fatigue strength, in order to meet the design objectives, PET-G material was selected as the printing material representing the properties summarized in Table 1.

Table 1. PET-G properties

Young modulus	2150 [MPa]
Tensile strength	50 [MPa]
Elongation at rupture	120 [%]
Density	1.27 [g/cm^3]

It is characterized by low hygroscopicity, it has been approved for contact with food, and for this reason, it has been used to manufacture dishes or bottles. As regards printing, it is characterized by a high level of adhesion during processing. This material behaves fine during mechanical processing and unlike PLA, PET-G printing is slower and more sensitive to parameter changes, which becomes immediately apparent in the printed detail, for example, in the form of lost transparency. The plastic is rigid and is used in prototyping products and verifying their mechanical strength. An additional advantage is the possibility to work in a wide temperature range (from -40ºC to +110ºC) and fine sliding properties, proven by a vast array of applications in sliding bearings. Glycol modification (suffix -G) increases Young's modulus.

To ensure the highest strength parameters, it was decided that the layers would be printed at 230ºC. A higher temperature (240ºC) should be applied to the first layer to ensure adhesion of the plastic to the heating table layer, a common problem that can lead to damaged prints. Printing the remaining layers at temperatures higher than 230ºC reduces the viscosity of the plastic as well as the dimensional accuracy of the printed part. As for printing speeds, the values of these parameters have been selected experimentally. In order to make sure that the layers of PET-G material fuse together, it is important to apply the correct speed. The speed cannot be too high or too low, as slow speed increases the time necessary to complete the print and can cause deformation caused by local overheating of the layer. The experimentally selected speeds are as follows: 30 mm/s for the outer walls and 50 mm/s for the inside. These parameters will help to maintain the consistency of the solid as well as the required dimensional accuracy.

Prosthesis modeling

The Skeleton model of the prosthesis was prepared in CAD Autodesk Inventor. First, it was necessary to prepare a simplified sketch, which included control dimensions and showed the kinematics of the device's operation, which will account for the limiting cases of the prosthesis. The geometric arrangement of the components on the plane helps to early predict the potential design problems such as where to set joint flexion limits or where to mount vibration dampers and other dynamic loads.

In order to make sure that the model functions properly, it was necessary to parameterize it. The next step involved setting limiting parameter values in Autodesk Inventor, from the smallest, allowing the model to be resolved, to the largest, which are optimal for the structure from a mechanical point of view. The parameters are linked directly to the skeleton model, which in turn translates these data into parameters for individual parts. Seven parameters were set relating to the length and three parameters relating to the angle.

Prosthesis' load

According to the chosen model, at rest the prosthesis is loaded evenly, i.e. each limb carries weight of ¼ of the dog's weight. This shows us that the forces and moments acting upon the prosthesis come from the weight and the response of the ground on which the dog is standing. According to the gait analysis, dynamic forces are acting upon the hindlimbs because the limb presses against the ground. Dynamic forces depend directly on the speed of the dog's movement, as well as the height to which the dog raises the limb. Depending on the speed of movement as well as the weight of the dog, the calculations will take into account an appropriate safety factor to compensate for the energy that is connected with the limb hitting the ground.

The following assumptions were made to determine the safety factor:

- approximation of the limb to a material point at the point of contact between the prosthesis and the ground;
- the ground does not absorb the impact energy;
- the mass of the material point is ¼ the mass of the dog m=6.25 kg;
- the maximum linear velocity of the limb from the initial to the final position is 2.78 m/s (about 10 km/h);
- the leg's elevation angle dφ=26º=0.4538 rad;
- the radius of the material point r=295.8 mm.

The analytically calculated coefficient is K=2.94.

Results of numerical calculations of the prosthesis

In order to complete numeric calculations, the following parameters were assumed:

- material is isotropic;
- main load F=179.92 N;
- secondary load F_{prot}=2.83 N, it is the force resulting from the mass of the prosthesis;
- the prosthesis is restrained at the contact surface of the prosthesis with the ground;
- the main load is applied to the surface where the endoprosthesis' mounting hole is located.

The finite element mesh was constructed from 10-node spatial (three-dimensional) elements. For static calculations, it was assumed that the mesh represented a characteristic size of 5 mm, with automatic compaction near notches. For models subject to shape analysis, the element size was reduced to 1 mm to obtain a higher resolution of the resulting shape.

During the process of designing the prosthesis, some of the dimensions were determined experimentally. The Shape Generator optimization module was used for further correction. The numerical calculations' results show us the maximum displacements of 1.848 mm and a minimum safety factor of 1.73. The actual load of the printed model points out to a low elastic deformability of the prosthesis, which is an undesirable phenomenon because of the transfer of loads coming from the ground's response to the endoprosthesis without their partial suppressing, which can in consequence cause damage to the prosthesis due to unpredictable rubbing at the junction or, in the worst case scenario, damage to the bone in the place where it is connected with the endoprosthesis.

The results of the calculations have been summarized in Table 2.

Table 2. Results of numerical calculations of the prosthesis

Reduced stresses at nominal load	31.4 [MPa]
Minimum safety factor	1.73
Maximum displacements	1.848 [mm]

The results of the calculations have been shown in the form of maps (Fig. 1).

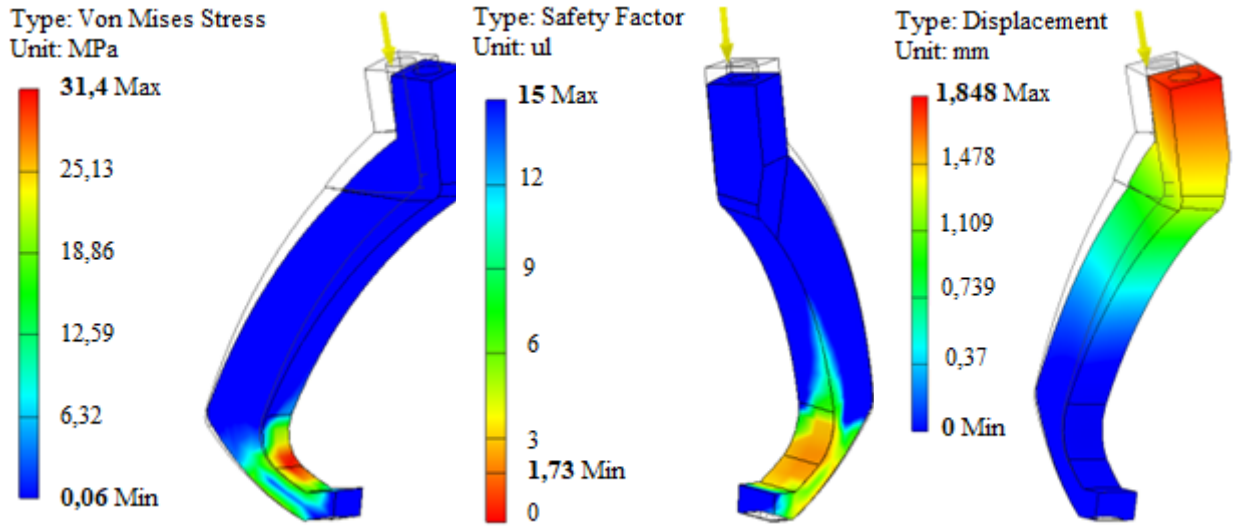

a) reduced stresses b) distribution of safety factor c) displacements

Fig. 1. Results of numerical calculations of the prosthesis

First, the optimization tool available in Autodesk Inventor was used, followed by numerical calculations, and in the end, the Shape Generator module was applied. The module has been designed to reduce the mass based on set criteria. Generating similar results as in strength calculations, it determines which finite element can be removed in order to slim down the structure to avoid damage.

For the purpose of optimization, an optimization area has been identified, defined as places of structural importance where it is not necessary to optimize the structure in order to slim it down. This step is important because the Shape Generator module is not able to recognize if the set part of the model is to fit and work with another detail or is normalized. In this project, this is the location where the prosthesis is connected and assembled with the endoprosthesis, as well as the place of contact of the prosthesis with the ground.

In this case, the criterion followed during the optimization in the module was stiffness maximization (Maximize Stiffness) and a weight reduction of 30-40%. A greater reduction is not necessary, since the weight of the prosthesis of ca. 200 g is almost imperceptible by the dog using it.

The precision of the operation was determined, as in every other process using the finite element method [16], [17]. Increased precision and accuracy increase the demand for computational resources and the time it takes for optimization to take place. The insufficient resolution will result in oversimplifications that can cause the structure to lose its stability, while a resolution that is too high increases computation time to several hours.

Optimization involves removing finite elements that do not carry loads or carry a relatively small value from the grid. Next, it reshapes it to distribute the stresses as evenly as possible. The result is a solid of an irregular shape caused by the removal of reduced finite elements. This function meets the condition of material continuity and the set conditions. The results of the optimization have been shown in Fig. 2.

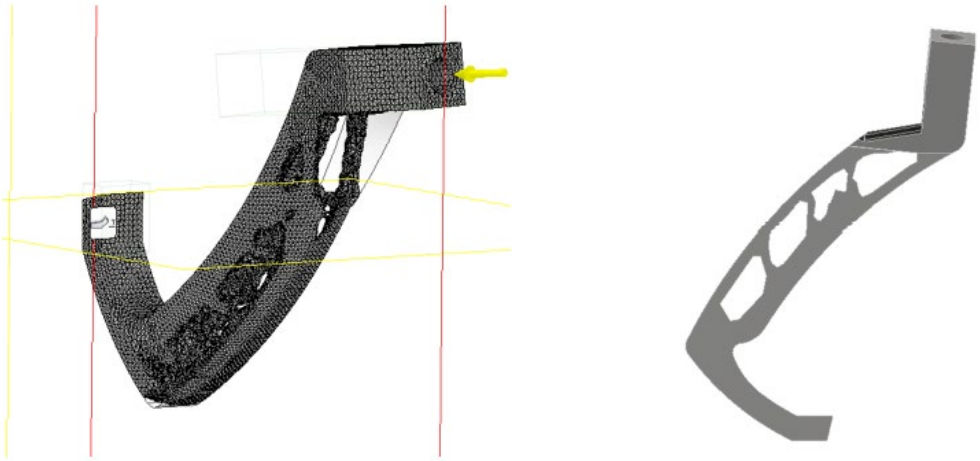

a) 3D model b) side view

Fig. 2. A solid generated after prosthesis optimization

The results of numerical calculations after optimization have been summarized in Table 3.

Table 3. Results of numerical calculations of the prosthesis after optimization

Reduced stresses at nominal load	33.12 [MPa]
Minimum safety factor	1.64
Maximum displacements	2.415 [mm]

The results of the prosthesis calculation after optimization have been shown in Fig. 3.

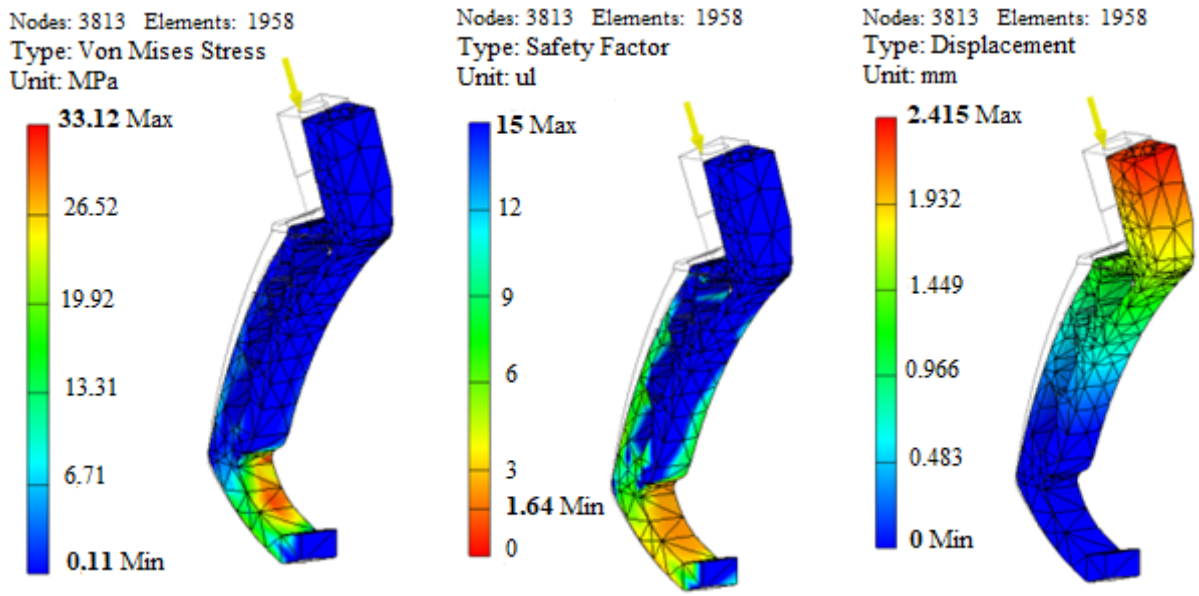

a) reduced stresses b) distribution of safety factor c) displacements

Fig. 3. Results of numerical calculations of the prosthesis after optimization

Empirical validation of numerical calculations of the prosthesis

To verify the numerical calculations, empirical validation of the calculations was performed. For this purpose, the printed prosthesis was mounted on an aluminum profile (Fig. 4). Followed by referential measurements. The prosthesis was loaded with cast iron weights of 17 kg (the weight of the tendon was omitted).

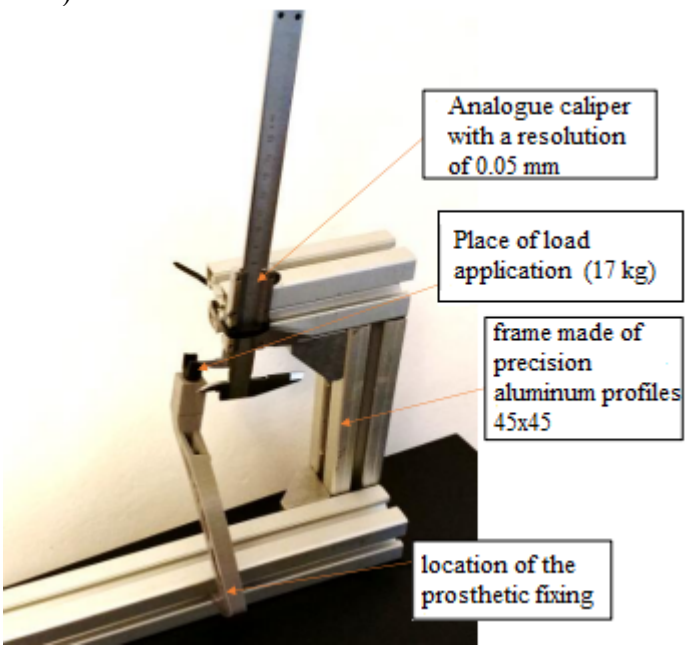

Fig. 4. Displacement measurements stand

Verifying the numerical calculations with the actual load applied, the relative errors of the maximum displacement measurement (against the numerical calculations) were calculated analytically, they were 94.8% for the prosthesis before the optimization process and 86.3% for the prosthesis whose shape was subject to the shape optimization process, respectively.

Conclusions

Based on the results of the conducted study, the following conclusions were drawn:

1. Excessive stiffness of the structure may cause the entire load to transfer to the endoprosthesis. Recurring loads with such stiffness cause the endoprosthesis and bones to carry increased loads from the ground, which may cause permanent damage to healthy parts of the dog's body.
2. Failure to install the endoprosthesis in the hole of the printed component correctly or improper matching of mating components may cause damage to the prosthesis because of the incorrect direction of loads. PET-G plastic is a relatively soft material and with poor metal-plastic mating, it will cause depravity of the latter.
3. The prosthesis is sensitive to the changing loads connected with the dog's weight. In this case, the dynamic load resulting from the dog's movement is three times greater than the static load. It means that each additional kilogram of the dog's weight will increase the basic dynamic load by about 30N.
4. To ensure optimal use of the material's properties, it is crucial to select the printer's plastic processing parameters. A printing temperature that is too low will prevent the layers from fusing properly and will eventually cause defusing, while a temperature that is too high will overheat the material or lead to incorrect application.

5. Optimization for the Maximize Stiffness criterion reduces maximum displacements and increases the safety factor through a more favorable distribution of loads within the solid. In addition to a more favorable distribution of stresses and displacements, optimization reduces the weight of the structure by 40%.
6. The relative measurement errors occur because the applied load differed from the nominal one by 8N. Secondly, it was assumed that the material would be isotropic. The third reason was that the strength of the printed element is lower than the strength of the same element made by injection molding, and, depending on the technology, is 60%-90% of the temporary endurance of the injected part. Another reason for the measurement error. The mounting method offered a different response than the assumed restraint of the contact surface of the detail with the substrate. Another reason for the error was a different load distribution along the layer lines, preventing a distribution that would match the numerical calculations. Additionally, another cause was the difference between Young's modulus used for the purpose of the calculations and the actual one. The sum of these errors makes up the total relative error of the measurement results.
7. In order to reduce the relative error, the material model should be changed to an anisotropic one, but in the case of FDM printed material, the number of material constants is so high that it cannot be implemented in the numerical calculation program that was used, so the assumed isotropy is a reasonable simplification in this case.

References

[1] Act of 21 August 1997 on the Protection of Animals (Journal of Laws of 1997, No. 111, item 724). In Polish

[2] M. Takayama-Ito, et al., Reduction of animal suffering in rabies vaccine potency testing by introduction of humane endpoints, Biologicals 46, pp. 38-45, 2017. https://doi.org/10.1016/j.biologicals.2016.12.007

[3] R. Bielawski, W. Rządkowski, M. P. Kowalik, M. Kłonica, Safety of aircraft structures in the context of composite element connection, Int. Rev. Aerosp. Eng. 13(5), pp. 159-164, 2020. https://doi.org/10.15866/irease.v13i5.18805

[4] R. Di Francia, V. Bizaoui, What if 3D Printing and Medicine had a dedicated Journal?, Ann. 3D Print. Med. 1, paper no 100007, 2021. https://doi.org/10.1016/j.stlm.2021.100007

[5] J. M. Liptak, W. S. Dernell, N. Ehrhart, M. H. Lafferty, G. J. Monteith, S. J. Withrow, Cortical Allograft and Endoprosthesis for Limb-Sparing Surgery in Dogs with Distal Radial Osteosarcoma: A Prospective Clinical Comparison of Two Different Limb-Sparing Techniques, Vet. Surg., 35 (6), pp. 518-533, 2006. https://doi.org/10.1111/j.1532-950X.2006.00185.x

[6] C. Sutton, et al., Titanium-nickel intravascular endoprosthesis: a 2-year study in dogs, Am. J. Roentgenol. 151 (3), pp. 597-601, 1988. https://doi.org/10.2214/ajr.151.3.597

[7] K. E. Mitchell, Metal endoprostheses for limb salvage surgery in dogs with distal radial osteosarcoma: evaluation of first and second generation metal endoprostheses and investigation of a novel endoprosthesis. 2017

[8] A. Timercan, V. Brailovski, Y. Petit, B. Lussier, B. Séguin, Personalized 3D-printed endoprostheses for limb sparing in dogs: Modeling and in vitro testing, Med. Eng. Phys. 71, pp. 17-29, 2019. https://doi.org/10.1016/j.medengphy.2019.07.005

[9] R. Mendaza-DeCal, S. Peso-Fernandez, J. Rodriguez-Quiros, Test of Designing and Manufacturing a Polyether Ether Ketone Endoprosthesis for Canine Extremities by 3D Printing, Front. Mech. Eng. 7, 2021. https://doi.org/10.3389/fmech.2021.693436

[10] S.-Y. Park et al., Custom-made artificial eyes using 3D printing for dogs: A preliminary study, PLoS One 15(11), paper no e0242274, 2020. https://doi.org/10.1371/journal.pone.0242274

[11] P. A. Manley, R. Vanderby, S. Kohles, M. D. Markel, J. P. Heiner, Alterations in femoral strain, micromotion, cortical geometry, cortical porosity, and bony ingrowth in uncemented collared and collarless prostheses in the dog, J. Arthroplasty, 10 (1), pp. 63-73, 1995. https://doi.org/10.1016/S0883-5403(05)80102-0

[12] E. Chisci, P. Dalla Caneva, i S. Michelagnoli, The "Dog Bone" Technique to Occlude a Branch Intentionally, Eur. J. Vasc. Endovasc. Surg. 61 (6), paper no 1035, 2021. https://doi.org/10.1016/j.ejvs.2021.02.032

[13] C. Ors, R. Caylak, E. Togrul, Total Hip Arthroplasty With the Wagner Cone Femoral Stem in Patients With Crowe IV Developmental Dysplasia of the Hip: A Retrospective Study, J. Arthroplasty 37 (1), pp. 103-109, 2022. https://doi.org/10.1016/j.arth.2021.09.007

[14] A. Santana, S. Alves-Pimenta, J. Martins, B. Colaço, M. Ginja, Imaging diagnosis of canine hip dysplasia with and without human exposure to ionizing radiation, Vet. J. 276, paper no 105745, 2021. https://doi.org/10.1016/j.tvjl.2021.105745

[15] G. Zhang, et. al., Frozen slurry-based laminated object manufacturing to fabricate porous ceramic with oriented lamellar structure, J. Eur. Ceram. Soc. 38 (11), pp. 4014-4019, wrz. 2018. https://doi.org/10.1016/j.jeurceramsoc.2018.04.032

[16] P. Różyło, H. Dębski, The Influence of Composite Lay-Up on the Stability of a Structure with Closed Section, Adv. Sci. Technol. Res. J. 16 (1), pp. 260-265, 2022. https://doi.org/10.12913/22998624/145156

[17] Z. Pater, P. Walczuk-Gągała, Conception of Hollow Axles Forming by Skew Rolling with Moving Mandrel, Adv. Sci. Technol. Res. J. 15(3), pp. 146-154, 2021. https://doi.org/10.12913/22998624/139134